

Mathematical Models of Spectral Density Function for Two-Domain Quasi-Random Structures,
Case Study of Organic Photovoltaics Active Layers.

Rabindra Dulal¹, Umar Farooq Ghumman², Joydeep Munshi³, Akshay Iyer², Aaron Wang¹,
Christoffer A. Masi¹, Wei Chen², Ganesh Balasubramanian³ and TeYu Chien^{1*}

¹*Department of Physics & Astronomy, University of Wyoming, Laramie, Wyoming, USA*

²*Department of Mechanical Engineering, Northwestern University, Evanston, IL, USA*

³*Department of Mechanical Engineering & Mechanics, Lehigh University, Bethlehem, PA, USA*

**E-mail: tchien@uwyo.edu*

Abstract

The Spectral Density Function (SDF) based analysis of the domain features for both experimental and simulated two-dimensional images are presented here. With the SDF used from the mathematical model developed, the domain distances and domain sizes for simulated data match well with the input verifying our model is correct and have more physical insights. Further using the SDF fitting for STM/S (Scanning Tunneling Microscopy and Spectroscopy) data, the domain size and domain distance are obtained. This SDF method for image analysis is not only restricted to STM images but can be used for AFM, SEM, TEM and all other type of two-dimensional images. This approach can be extended to SAXS data analysis as well.

Introduction:

Owing to the various properties like environment friendly, flexibility, light weight, low cost of production organic photovoltaic (OPVC) has drawn much attention as one of the most promising candidate for next generation photovoltaics [1] [2] [3]. It has been shown that the Bulk heterojunction (BHJ) architecture is the key factor to ensure the high efficiency and compensate the short exciton length of the OSC. It is reported that with bulk heterojunction architecture the OSC has domain like features corresponding to donor and acceptor molecules [1] [4]. Organic photovoltaic study has gained importance from not only on experimental approach but in computational approach too using Coarse Grained Molecular simulations (CGMD) and other computational techniques [4–9]. It is widely accepted that the OPVC active layer has two domain structure but the domain properties like the domain distance and domain size are not explored well yet. With the most studied organic semiconductor's P3HT and PCBM, here we study the domain features using SDF.

SDF has been a unique representation from physics point of view [4] [5]. Mathematically, SDF is calculated as the radial average of the squared magnitude of Fourier spectrum. SDF function fitting gives the information about the real space features like the domain size and the domain distance through the Fourier transform. Previous work has proven that SDF is an essential tool for the characterization of the heterogeneous microstructural features in the spatial space. Reconstruction of the original microstructure has been achieved using SDF function [4] [10]. Spectral Density function used for the reconstruction of various Quasi-Random Nanostructured Material System illustrate the various physical phenomena like the Light trapping in solar cells, various biological and natural phenomena [11]. The use of SDF to understand the Nano structured

Material System is growing. Hyperuniform two phase material constructed with the SDF showed novel and optimal transport and electromagnetic properties [12]. Similarly, studies on the disordered hyperuniform many body systems for two-phase media suggests a relation between autocovariance function and associated spectral density [13] [14]. SDF based analysis and fitting of the nanostructured material system data is not a new practice [15] [16]. But in most of the studies the SDF fitting function used are chosen randomly and hence doesn't have much physical insights into the material system. Thus, to have more physical insights, here we have developed a mathematical model of the SDF that can be used for all two-dimensional and three-dimensional Small Angle X-ray Scattering (SAXS) data.

Here we use the SDF approach for simulated data and Scanning Tunneling Microscopy (STM) data. STM is widely used technique in material science, Organic Photovoltaic, Polymer physics, Nanostructured Material system to understand the atomic scale mapping of those material [9] [17]. STM has unique tool called dI/dV mapping that can measure electronic Local Density of States (LDOS) of the nanostructured material system which represents the electronic LDOS for two domain, acceptor and donor semiconductors. Organic Photovoltaic are also an example of quasi random nanostructured material system. Understanding of STM data of Organic photovoltaic using SDF is an unique approach which gives the domain size, the domain distance in the K space.

Similarly, SAXS techniques are widely used in polymer physics, material science for the characterization of the nanostructured material system. Developments of the experimental and the computational tools have made it easier for the characterization of Nano Structured Material Systems [18]. The mathematical model we developed here for the three dimensional dot feature is similar to what people have already reported for fitting the SAXS data [19]. Thus, our approach

of SDF based analysis works for SAXS data as well. Further in this paper we present the simulation of gaussian function, step function and compute the SDF that can represent the real STM data of photovoltaic and correlate the simulation and the real data.

Sample Preparation and STM Measurements:

Solutions containing 20 mg P3HT/ 1 mL of chlorobenzene (purity \geq 99.5%, sigma-aldrich) and 20 mg PCBM/ 1 mL of chlorobenzene is prepared and mixed in 1:1, 2:1 and 1:2 weight ratio. The solutions were spin coated onto the Si (100) substrate with 1050 rpm speed for 1 minute. The films containing P3HT: PCBM/Si (100) were annealed at 100°C for 20 minutes for 1:1 ratio, at 150°C for 5 min for 2:1 weight ratio and at 150°C for 5 min for 1:2 weight ratio inside the glove box. The sample mounted on a sample plate with stainless steel clamps for in-situ fracturing in UHV environment prior to the XSTM/S (Cross-Sectional Scanning Tunneling Microscopy and Spectroscopy) measurements [9] [20]. The sample is then fractured in UHV from the side so that the film region is not affected. Finally, the cross-sectional fresh fractured Si and P3HT: PCBM film region is scanned inside the scanning chamber of STM.

STM/S is a technique that utilizes quantum tunneling effects across the tip–sample junction to perform topographical imaging and electronic Local Density of States (LDOS) with atomic resolution [20]. The active layers were imaged with XSTM/S [20], to image OPVCs [4,9] and perovskite solar cells [21]. Cleaving and fracturing of the sample were applied to generate the fresh surface on Si for measurements as organic solar cell active layer degrade upon sputtering and annealing of the active layer.

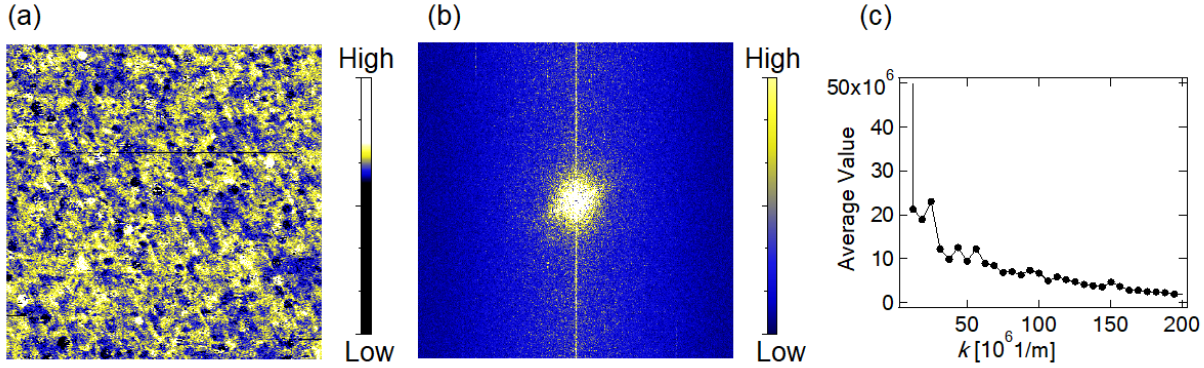


Figure 1(a) STM dI/dV mapping of images of size 160 nm. (b) Fourier transform of (a). (c) Radial Average curve (SDF) of (a).

Figure 1 (a) shows the local electronic density of states mapping (LDOS) represented by two contrast color showing donor rich region i.e P3HT rich region and PCBM rich region. Fig. 1(b) is the Fourier transform of fig. 1(a) which is isotropic and fig. 1(c) is the SDF curve obtained by the radial average of fig 1(b) showing peak like features representing the domain information. The peak features in the SDF curve corresponds to the domain distance whereas the overall decay is represented by the domain size.

Result and Discussion

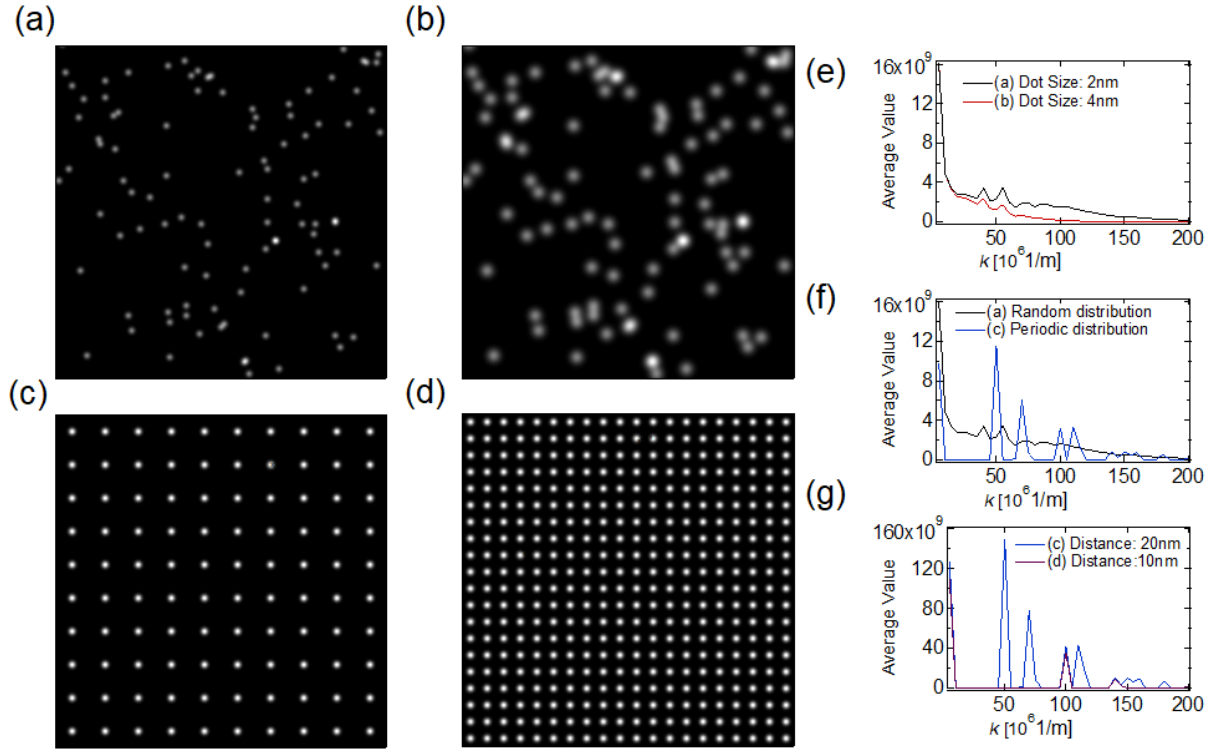


Fig. 2. Simulation of 100 dot features with image size 200 nm X 200 nm using the gaussian function; (a) with the FWHM as 2 nm, (b) with the FWHM as 4 nm, (c) with FWHM as 2nm and periodic separation of gaussian of 20 nm and , (d) Simulation of 400 dot features with image size 200 nm X 200 nm using the gaussian function with FWHM as 2nm and periodic separation of gaussian of 10 nm (e) SDF curve of (a) and (b). (f) SDF curve of (a) and (c). (g) SDF curve of (c) and (d).

The dI/dV mapping of P3HT: PCBM looks like a Gaussian function, so to understand the SDF curve and physical meaning of it we try to see the simulation of multiple gaussian and see how the SDF evolves. Figure 2(a)-(d) shows the simulations of the random same size, different size and periodic dot features. Figure (e) shows that the SDF function changes with the size of the dot features where red curve with 4 nm dot size decays to 0 faster as compared to one with 2 nm. This shows larger the size of the dot features, larger is the decay rate and thus the SDF curves goes to

0 faster. Figures (f) demonstrate that the SDF function changes with the periodicity. The blue curve in the fig. 2(f) shows peak features corresponding to the periodic distance of 20 nm in the fig. 2(c). Fig. 2(g) shows how the SDF function changes with the different distance distribution. Both curves in fig. 2(g) shows peak features corresponding to their periodicity as seen in fig. 2(c), periodic distance of 20 nm and 2(d) with periodic distance of 10 nm. Thus, it is observed that for SDF function, the decay rate, shape of the function, the peak feature is determined by the domain size, domain distance and the domain texture.

Mathematical Basis:

For further understanding of the SDF function and get more information about the domain features, we did some mathematical derivation for the SDF function in 1D, 2D and 3D.

1D Gaussian:

First, we start with the two one-dimensional Gaussian function given by:

$$f(x) = \sum_{i=1}^2 e^{-(x-x_i)^2/c^2}$$

Where c is the size of Gaussian, x_i is the position of the Gaussian.

Use the Fourier transform relation:

Fourier Transform $F(k) = \int_{-\infty}^{\infty} f(x) e^{-2\pi i k x} dx$ to calculate the FFT as shown below:

$$F(k) = \sum_{i=1}^2 e^{-2\pi i x_i k} e^{-c^2 \pi^2 k^2}$$

For a one-dimensional Gaussian the SDF is given by the amplitude square of the FFT. For two one-dimensional Gaussian, the SDF is given by:

$$SDF = 2\pi c^2 e^{-2c^2\pi^2 k^2} (1 + \cos (2\pi k d)) \dots \quad (1)$$

Where d is the distance between the Gaussian.

2D Gaussian:

For two dimensional Gaussian with two Gaussian as,

$$f(x, y) = \sum_{i=1}^2 e^{-((x-x_i)^2 + (y-y_i)^2)/c^2}$$

Where c is the size of the Gaussian, (x_i, y_i) give the position of the Gaussian in 2D.

Using the Fourier transform relation:

Fourier Transform $F(k) = \int_{-\infty}^{\infty} \int_{-\infty}^{\infty} f(x, y) e^{-2\pi i k_x x} e^{-2\pi i k_y y} dx dy$ to calculate the FFT as:

$$F(k) = \sum_{i=1}^2 e^{-c^2 \pi^2 (k_x^2 + k_y^2)} e^{-2\pi i (k_x x_i + k_y y_i)}$$

For a two-dimensional Gaussian the SDF is given by radial average of the amplitude square of the FFT. The amplitude square of the FFT is calculated as:

$$|F(k)|^2 = 2\pi^2 c^4 e^{-2\pi^2 c^2 K^2} [1 + \cos\{2\pi(k\Delta r \cos\theta)\}]$$

where $\vec{k} \cdot \vec{\Delta r} = \{k_x(x_1 - x_2) + k_y(y_1 - y_2)\}$

Using the following relation to calculate the SDF:

$$SDF = \frac{\int_0^{2\pi} |F(k)|^2 d\theta}{2\pi}$$

Finally, the SDF is given by:

$$SDF = 2\pi^2 c^4 e^{-2k^2\pi^2 c^2} (1 + J_0(2\pi k d)) \dots \quad (2)$$

Where J_0 is the Bessel function of first kind, d is the distance between the Gaussian.

3D Gaussian:

For three dimensional Gaussian with two Gaussian as.

$$f(x, y, z) = \sum_{i=1}^2 e^{-((x-x_i)^2 + (y-y_i)^2 + (z-z_i)^2)/c^2}$$

Where c is the size of the Gaussian, (x_i, y_i, z_i) give the position of the Gaussian in 3D.

Using the Fourier transform relation:

$$\text{Fourier Transform} \quad F(k) = \int_{-\infty}^{\infty} \int_{-\infty}^{\infty} \int_{-\infty}^{\infty} f(x, y) e^{-2\pi i k_x x} e^{-2\pi i k_y y} e^{-2\pi i k_z z} dx dy dz \quad \text{to}$$

calculate the FFT as:

$$F(k) = \sum_{i=1}^2 \pi^{3/2} c^3 e^{-c^2 \pi^2 (k_x^2 + k_y^2 + k_z^2)} e^{-2\pi i (k_x x_i + k_y y_i + k_z z_i)}$$

For a three-dimensional Gaussian the SDF is given by radial average of the amplitude square of the FFT. The amplitude square of the FFT is calculated as:

$$|F(k)|^2 = 2\pi^3 c^6 e^{-2\pi^2 c^2 k^2} [1 + \cos\{2\pi(k\Delta r \cos\theta)\}]$$

Where $\vec{k} \cdot \vec{\Delta r} = \{k_x(x_1 - x_2) + k_y(y_1 - y_2)\}$

Using the following relation to calculate the SDF:

$$SDF = \frac{\int_0^\pi \int_0^{2\pi} |F(k)|^2 k \sin \theta d\theta dk \Phi}{4\pi k^2}$$

Finally, the SDF is given by:

Where d is the distance between the Gaussian

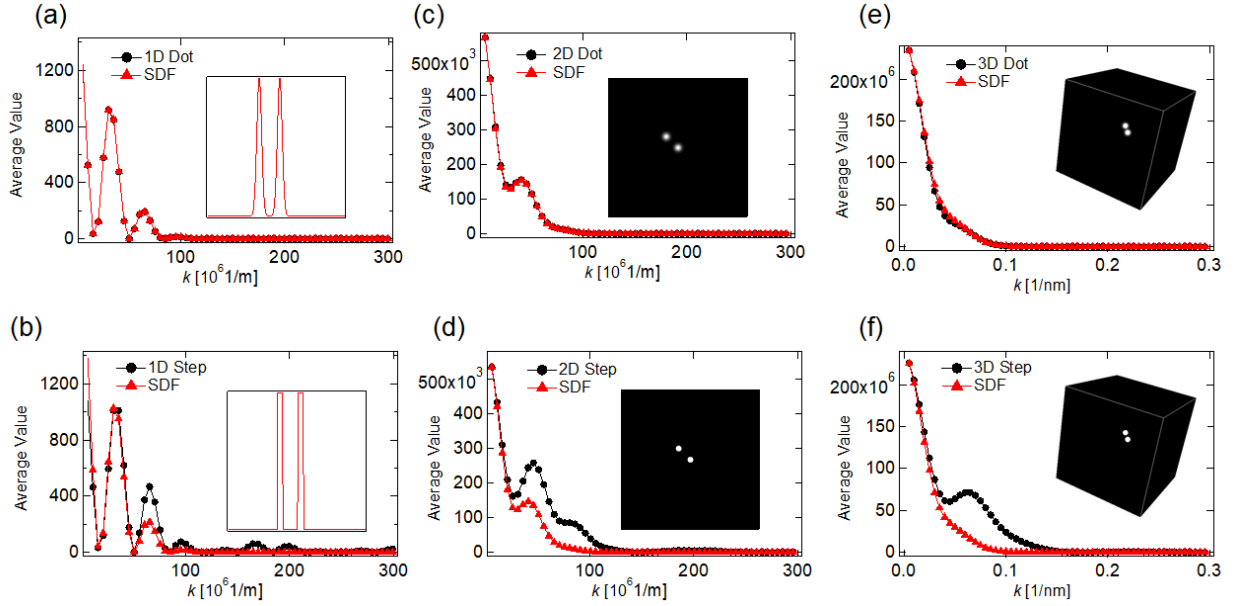


Fig.3, Inset: Simulation of two gaussian each with size 5 nm in 200 nm window: (a) two one dimensional Gaussian, (b) two one dimensional step function, (c) two two-dimensional Gaussian, (d) two two-dimensional step function, (e) two three-dimensional Gaussian, (f) two three-dimensional step function. Fig3(a)-(f) SDF curve is represented by black line and the fitting with the mathematical equation developed is the red line.

From figures 3(a), (c) and (e), it is seen that the mathematical SDF and the experimental SDF matches well for 1D, 2D and 3D dot features. The peak features in the SDF curve corresponds to the input domain distance and the decay features corresponds to the domain size which is the size of the dot features. From figures 3(b), it is seen that the mathematical SDF and the experimental SDF matches well for 1D step function except few points. Similarly, figure 3(d) also shows that the mathematical SDF and experimental SDF have similar overall trend whereas from figure 3(f), there is some deviations for the step function. This might be because the method we developed is for dot features not for the step function. This shows our method works not only for dot features, it works for 1D and 2D step function. To further broadening our understanding to multiple dot

features, we do simulation of 100 of dot features in 2D. With the simulations of 100 of dot features, we need to modify our math to convolute all the possible sizes and distances.

Convolution for same size:

For n two-dimensional same size Gaussian, the sum is given as:

$$Sum = \pi^2 c^4 e^{-2k^2 \pi^2 c^2} (n + \sum_{i=1}^{\frac{n^2-n}{2}} 2J_0(2\pi k d_i))$$

For convolution:

$$\text{Fitting Equation: } F(k) = e^{-\frac{(c-\bar{c})^2}{\sigma_c^2}} (A_1 c^4 e^{-2k^2 \pi^2 c^2}) \int_0^\infty e^{-\frac{(d-\bar{d})^2}{\sigma_d^2}} (1 + J_0(2\pi k d)) dd \quad \dots \dots \dots (4)$$

where, \bar{c} is the average domain size, σ_c is the S.d of the domain, \bar{d} is the average domain distance, σ_d is the S.d of the domain distance.

Convolution for different size:

For n two-dimensional different size Gaussian, the sum is given as:

$$SDF_n = Sum = \pi^2 \sum_{i=1}^n c_i^4 e^{-2\pi^2 c_i^2 k^2} + 2\pi^2 \sum_{i=2}^n \sum_{j=1}^{i-1} c_i^2 c_j^2 e^{-\pi^2 k^2 (c_i^2 + c_j^2)} J_0(2\pi k d_{i,j})$$

For convolution:

$$\text{Fitting Equation: } F(K) = A(\pi^2 n G(cc) + 2\pi^2 \frac{n^2-n}{2} (F(cc))^2 E(J_0)) \dots \dots \dots (5)$$

$$E(J_0) = \frac{\int_0^\infty e^{(\frac{-(d-\bar{d})^2}{(d^{w[3]} b)^2})} J_0(2\pi k d) dd}{\int_0^\infty e^{(\frac{-(d-\bar{d})^2}{(d^{w[3]} b)^2})} dd}$$

$$F(cc) = \frac{\int_0^\infty (e^{(\frac{-(c-\bar{c})^2}{(\sigma_c)^2})} c^2 e^{-k^2 \pi^2 c^2} dc)}{\int_0^\infty e^{(\frac{-(c-\bar{c})^2}{(\sigma_c)^2})} dc}$$

$$G(cc) = \frac{\int_0^{\infty} (e^{\frac{-(c-\bar{c})^2}{(\sigma_c)^2}} c^4 e^{-2k^2\pi^2 c^2} dc)}{\int_0^{\infty} e^{\frac{-(c-\bar{c})^2}{(\sigma_c)^2}} dc}$$

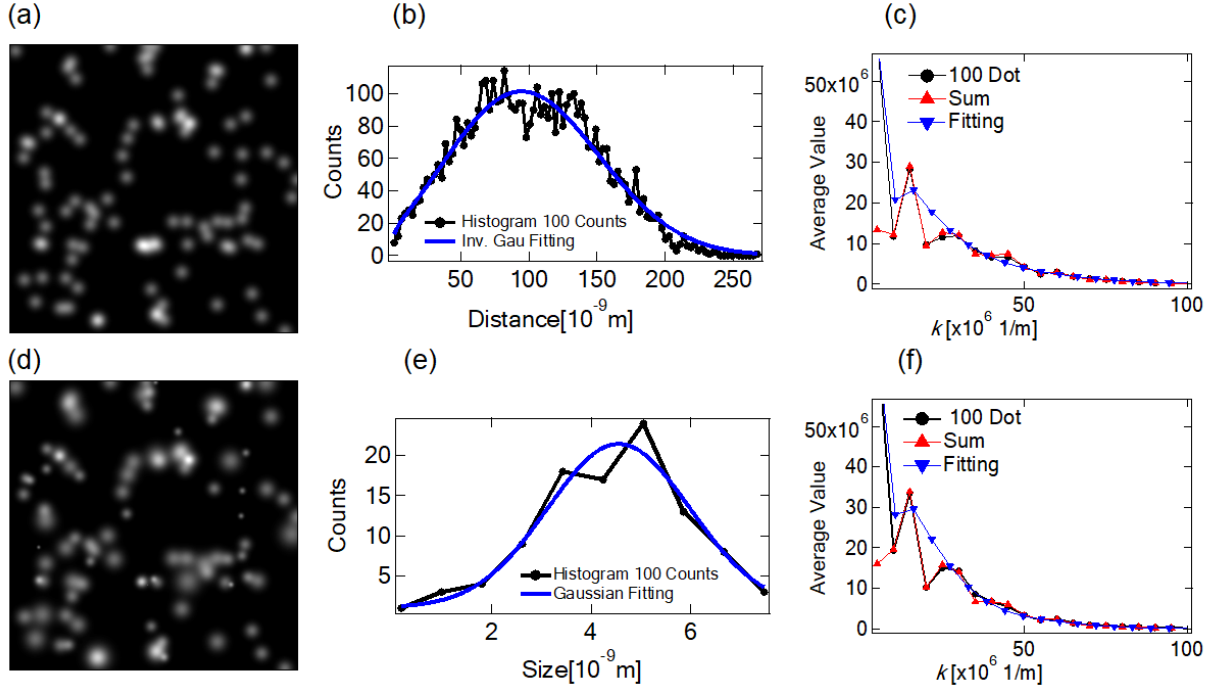


Fig. 4(a) Simulation of 100 dot features using the gaussian function and keeping the FWHM as 4.83 nm and image size 200 nm X 200 nm. (b) Distance Histogram for all the dot features from fig(a) represented by black line and fitting represented by blue line. (c) SDF, sum curve and the convolution fitting represented by the black, red and blue curve respectively. (d) Simulation of 100 dot features of different size using the gaussian function and keeping the average size as 4.83 nm and image size 200 nm X 200 nm. (e) Size Histogram for all the dot features from fig(d) represented by black line and fitting represented by blue line. (f) SDF, sum curve and the convolution fitting represented by the black, red and blue curve respectively.

Fig 4(c), the SDF convolution and sum from fig 4(a) is fitted with the equation 4, the convolution for the same size. Similarly, fig 4(f), the SDF convolution and sum from fig 4(d) is fitted with equation 5, the convolution for different size. With the convolution fitting we extract the

information about the domain size and the domain distance, like the input as seen in table 1. While fitting the different size SDF with the different size convolution, the s.d of the size has a large error $\sigma_c = -6.3e^{-5} \pm 6.9e^{-5}$ as seen in table 1. Taking this into account, different size image is fitted with same size convolution which improved the fitting as shown in table 1. Thus, this proves that our math works well for 100's of dot features. This method of fitting two-dimensional data is an unique approach with the correct physical interpretation of the equation. Thus, with this SDF based approach, the domain distances and the domain sizes can be obtained precisely.

Further as the convolution equation (4) and (5) has n, w terms that doesn't have much physical significance, we run 100's of simulation to determine the value of w. With 100's of simulations for different dot sizes, the range of w is found to be from 0.04 ± 0.02 - 0.06 ± 0.01 . Then we run 20

Input	Histogram fitting $f(d) = Ae^{\frac{-(d-\bar{d})^2}{(d^w b^2)}}$	Convolution (same Size)	Convolution (Diff. Size)
Same Size $c: 4.83 \text{ nm}, \bar{d}: 102 \text{ nm}$	$\bar{d} = 94.5 \text{ nm} \pm 1.6 \text{ nm}$ $b = 154.7 \text{ nm} \pm 53.3 \text{ nm}$ $w = 0.08 \pm 0.04$	$\bar{d} = 85.6 \text{ nm} \pm 3.7 \text{ nm}$ $b = 147.3 \text{ nm} \pm 228.2 \text{ nm}$ $w = 0.10 \pm 0.15$ $n = 7.52 \times 10^3 \pm 1.17 \times 10^3$ $\bar{c} = 4.37 \text{ nm} \pm 0.63 \text{ nm}$	
Diff Size $\bar{c}: 4.83 \text{ nm}, \bar{d}: 102 \text{ nm}$		$\bar{d} = 85.2 \text{ nm} \pm 2.9 \text{ nm}$ $b = 79.3 \text{ nm} \pm 169.1 \text{ nm}$ $w = 0.03 \pm 0.22$ $n = 0.18 \times 10^3 \pm 6.27 \times 10^3$ $\bar{c} = 4.67 \text{ nm} \pm 1.13 \text{ nm}$	$\bar{d} = 85.6 \text{ nm} \pm 3.6 \text{ nm}$ $b = 105.9 \text{ nm} \pm 220.0 \text{ nm}$ $w = 0.06 \pm 0.21$ $n = 7.52 \times 10^3 \pm 1.17 \times 10^3$ $\bar{c} = 4.62 \text{ nm} \pm 1.21 \text{ nm}$ $\sigma_c = -6.3 \times 10^3 \text{ nm} \pm 6.9 \times 10^3 \text{ nm}$ $n = 0.94 \times 10^3 \pm 3.33 \times 10^3$

Table 1: Fitting results for fig 4(c) and 4 (f) using the convolution equation 4 and 5.

convolution fitting fixing w and n and found the value of w to be 0.04 and n to be 100 which is close to our input parameter (details in supporting information). This modified fitting equation is used to fit the SDF obtained from the STM data.

STM data Convolution fitting:

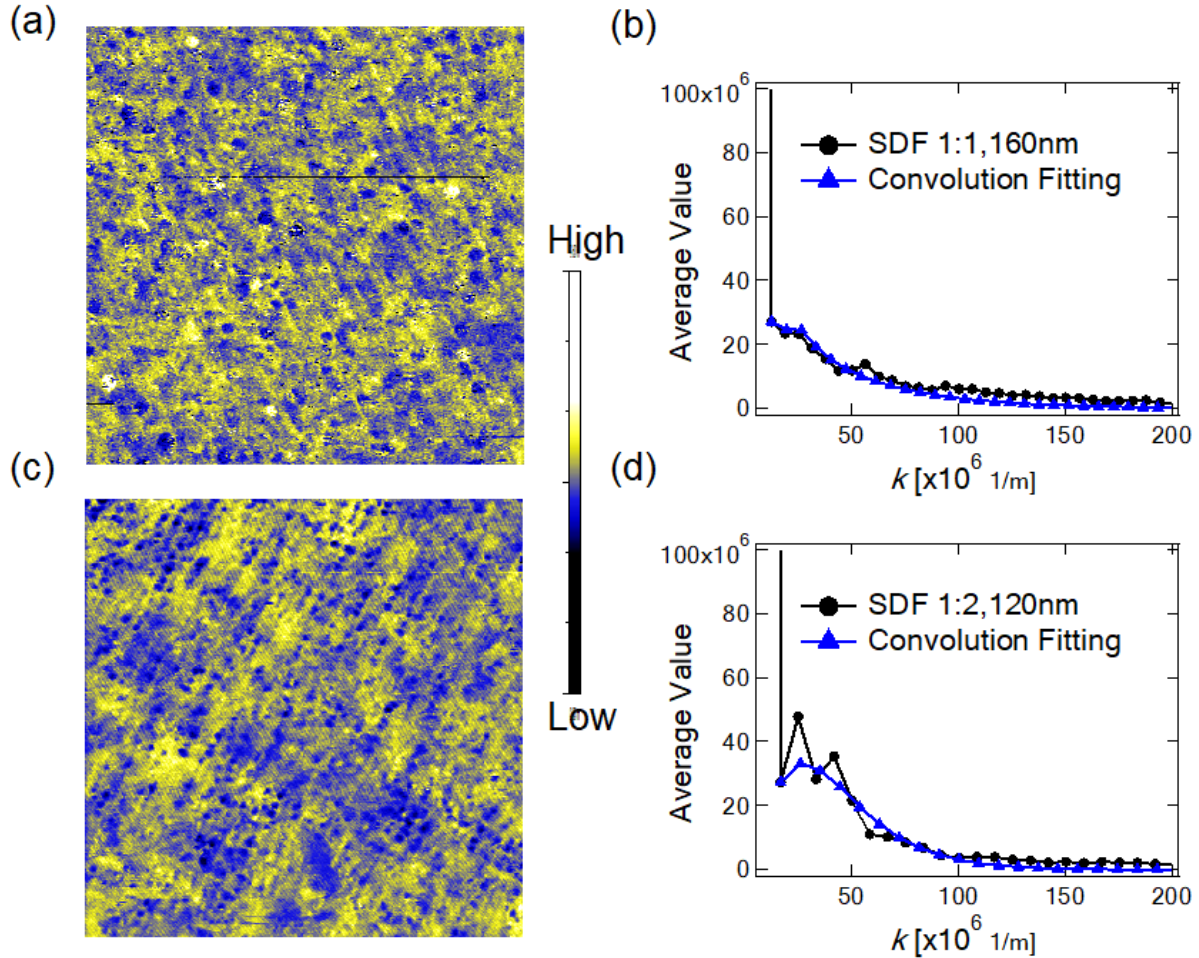


Fig. 5. STM dI/dV mapping: (a) size 160 nm with P3HT:PCBM in the ratio 1:1, (c) size 120 nm with P3HT:PCBM in the ratio 1:2, Fig (b), (d) are Radial Average (SDF) of (a) and (c) respectively with the black line representing the SDF and blue line representing the convolution fitting

Using the convolution equation for the same size gaussian i.e equation 4, we fit the STM data assuming the same average size of the domain. We fit the SDF obtained for the STM data from the second point as the first point has much higher intensity. With the fitting results, we obtained the domain size and the domain distance information tabulated in table 2.

Input	Convolution (same Size)
P3HT:PCBM 1:1 ratio, 160 nm	$\bar{d} = 38.3 \text{ nm} \pm 3 \text{ nm}$ $b = 64.1 \text{ nm} \pm 8.0 \text{ nm}$ $\bar{c} = 3.0 \text{ nm} \pm 0.3 \text{ nm}$
P3HT:PCBM 1:2 ratio, 120 nm	$\bar{d} = 57.7 \text{ nm} \pm 0.4 \text{ nm}$ $b = 60.8 \text{ nm} \pm 2.0 \text{ nm}$ $\bar{c} = 2.78 \text{ nm} \pm 0.09 \text{ nm}$

Table 3: Fitting results from SDF fitting in fig. 14(b) and (d) using the convolution equation 8 for same size convolution.

With the mathematical SDF fitting model, the domain distance and domain size for two STM images were found to be $38.3 \text{ nm} \pm 0.30 \text{ nm}$, $3.0 \text{ nm} \pm 0.3 \text{ nm}$ and $57.66 \text{ nm} \pm 0.04 \text{ nm}$, $2.72 \text{ nm} \pm 0.009 \text{ nm}$ respectively as shown in table 2. Thus, our SDF approach worked well for the extraction of the important parameter for two-dimensional images for both simulated and experimental data. This approach can further be applied to AFM, STM, SEM and other two-dimensional images as well.

Conclusion

In summary, the SDF mathematical model developed for 1D, 2D and 3D dot features works well with the simulated data. The domain size and domain distance information extracted from the SDF fitting using the mathematical SDF model matches well with input. This mathematical SDF model developed not only gives the domain information but also have physical insights about the fitting function used. Further, with the mathematical SDF fitting model, the domain distance and domain size for two STM images were found to be $38.3 \text{ nm} \pm 0.30 \text{ nm}$, $3.0 \text{ nm} \pm 0.3 \text{ nm}$ and $57.66 \text{ nm} \pm 0.04 \text{ nm}$, $2.72 \text{ nm} \pm 0.009 \text{ nm}$ respectively as shown in table 2. Finally, this SDF fitting method

for image analysis is not only restricted to STM images but can be used for AFM, SEM, TEM and all other type of two-dimensional images and can further be applied for SAXS data analysis with physical meaning of the parameters used in the equation.

Funding Sources

This work was supported by the National Science Foundation (NSF) under Award Nos. CMMI-1662435, 1662509 and 1753770.

Notes

The authors declare no competing financial interest.

ACKNOWLEDGMENT

This work was supported by the National Science Foundation (NSF) under Award Nos. CMMI-1662435, 1662509 and 1753770.

Reference:

- [1] P. R. Berger and M. Kim, *J. Renew. Sustain. Energy* **10**, 013508 (2018).
- [2] H. Zhang, H. Yao, J. Hou, J. Zhu, J. Zhang, W. Li, R. Yu, B. Gao, S. Zhang, and J. Hou, *Adv. Mater.* **30**, 1 (2018).
- [3] H. H. Gao, Y. Sun, X. Wan, X. Ke, H. Feng, B. Kan, Y. Wang, Y. Zhang, C. Li, and Y. Chen, *Adv. Sci.* **5**, 1 (2018).
- [4] U. F. Ghumman, A. Iyer, R. Dulal, J. Munshi, A. Wang, T. Chien, G. Balasubramanian, and W. Chen, *J. Mech. Des.* 1 (2018).

- [5] U. F. Ghumman, A. Iyer, R. Dulal, J. Munshi, A. Wang, T. Chien, G. Balasubramanian, and W. Chen, in *ASME IDETC/CIE* (2018), p. V02BT03A015-V02BT03A015.
- [6] J. Munshi, U. Farooq Ghumman, A. Iyer, R. Dulal, W. Chen, T. Chien, and G. Balasubramanian, *Comput. Mater. Sci.* **155**, 112 (2018).
- [7] J. Munshi, U. F. Ghumman, A. Iyer, R. Dulal, W. Chen, T. Chien, and G. Balasubramanian, *J. Polym. Sci. Part B Polym. Phys.* **57**, 895 (2019).
- [8] A. Iyer, R. Dulal, Y. Zhang, U. F. Ghumman, and T. Chien, ArXiv:1908.07661 (n.d.).
- [9] R. Dulal, A. Iyer, U. F. Ghumman, J. Munshi, A. Wang, G. Balasubramanian, W. Chen, and T. Chien, *ACS Appl. Polym. Mater.* **2**, 335 (2020).
- [10] R. Bostanabad, Y. Zhang, X. Li, T. Kearney, L. C. Brinson, D. W. Apley, W. K. Liu, and W. Chen, *Prog. Mater. Sci.* **95**, 1 (2018).
- [11] S. Yu, Y. Zhang, C. Wang, W. Lee, B. Dong, T. W. Odom, C. Sun, and W. Chen, *J. Mech. Des.* **139**, 071401 (2017).
- [12] D. Chen and S. Torquato, *Acta Mater.* **142**, 152 (2018).
- [13] S. Torquato, *J. Phys. Condens. Matter* **28**, (2016).
- [14] C. E. Zachary and S. Torquato, *J. Stat. Mech. Theory Exp.* **2009**, P12015 (2009).
- [15] S. Yu, C. Wang, Y. Zhang, B. Dong, Z. Jiang, and X. Chen, *Sci. Rep.* **1** (2017).
- [16] W. K. Lee, S. Yu, C. J. Engel, T. Reese, D. Rhee, W. Chen, and T. W. Odom, *Proc. Natl. Acad. Sci. U. S. A.* **114**, 8734 (2017).
- [17] J. Munshi, R. Dulal, T. Chien, W. Chen, and G. Balasubramanian, *ACS Appl. Mater.*

Interfaces **11**, 17056 (2019).

- [18] J. Ilavsky and P. R. Jemian, *J. Appl. Crystallogr.* **42**, 347 (2009).
- [19] R. Erler, A. F. Thu, S. Sokolov, T. T. Ahner, K. Rademann, F. Emmerling, and R. Krahnert, *ACS Nano* **4**, 1076 (2010).
- [20] A. Wang and T. Chien, *Phys. Lett. A* **382**, 739 (2018).
- [21] A. J. Yost, A. Pimachev, C. C. Ho, S. B. Darling, L. Wang, W. F. Su, Y. Dahnovsky, and T. Chien, *ACS Appl. Mater. Interfaces* **8**, 29110 (2016).